

USE OF CFD TO DETERMINE EFFECT OF WIRE MATRIX INSERTS ON CRUDE OIL FOULING CONDITIONS

M. Yang and B.D. Crittenden*

Department of Chemical Engineering, University of Bath, Bath, UK, BA2 7AY

*corresponding author: B.D.Crittenden@bath.ac.uk

ABSTRACT

Crude oil fouling rates are strongly affected by both local surface temperature and local surface shear stress. The use of in-tube inserts (such as hiTRAN[®]) in heat exchangers has been shown to be effective in mitigating crude oil fouling whilst at the same time enhancing heat transfer. However, the introduction of inserts means that there will be axial and radial distributions of both local shear stress and local heat transfer coefficient between the repeating insert-wall contact points, which could mean that there will be local variations in fouling rate. Whilst estimation of local shear stresses and film heat transfer coefficients is facile for bare round tubes, this is no longer the case for tubes fitted with inserts. Accordingly, this paper describes a possible solution to the design challenge using CFD simulation, the output of which is the temperature and velocity distributions in a three dimensional geometry of the fluid flow in a tube fitted, for example, with a hiTRAN[®] insert. A simple algorithm is then described for calculating the overall heat transfer coefficient based on the resulting temperature distribution along the wall of the tube. Simulated values of the overall heat transfer coefficient are then compared with those obtained by experiment, showing that there is good agreement, thereby indicating that predicted local values are accurate. Use of CFD in fouling applications now allows the prediction of local conditions when inserts are used and hence can be used to predict if, and where, fouling might occur.

INTRODUCTION

hiTRAN[®] in-tube inserts have been shown to be effective in mitigating crude oil fouling and enhancing heat transfer (Crittenden et al., 1993; Ritchie and Droegemueller 2008; Ritchie et al., 2009). Increasing interest in their use in such applications is being shown by the oil industry (Krueger and Pouponnot, 2009) as well as by the water industries (Bott 2001; Wills et al., 2000). A good review of applications and benefits of tube inserts in heat exchangers is provided by Ritchie and Droegemueller (2008).

Nonetheless, the use of inserts creates a challenge in the design of a heat exchanger, due to insufficient understanding of the fouling behaviour and lack of practical methods for estimation of some critical design parameters, the heat transfer coefficient in particular. Fouling of the heat

exchanger depends, amongst other things, on two key operational parameters, namely the wall shear stress and the surface temperature. In previous work (Yang et al., 2009; Yang and Crittenden, 2011), a CFD approach was developed to reveal the wall shear stress distribution for tubes with and without inserts fitted, and hence to develop a suitably modified, but unified, fouling model to predict the fouling rate and threshold conditions for both cases. The surface temperature distribution in the case of tubes fitted with inserts is more complicated than that for a bare tube. Whilst the heat transfer coefficient is easily calculated for bare round tubes using, for example, the Dittus-Boelter method, such a simple procedure cannot be used when hiTRAN[®] inserts are fitted. The objective of this work, therefore, is to determine whether CFD simulation can offer a possible solution to this challenge such that the surface temperature distribution and the heat transfer coefficient can be estimated for use in evaluating the fouling potential and hence in the design of a heat exchanger fitted with tubes containing inserts. The averaged heat transfer coefficient resulting from the model will be compared with that obtained from experiments.

EXPERIMENTS

Details of the experimental rig (shown in Figure 1), the crude oil, the procedure and results with bare tubes are provided by Crittenden et al. (2009).

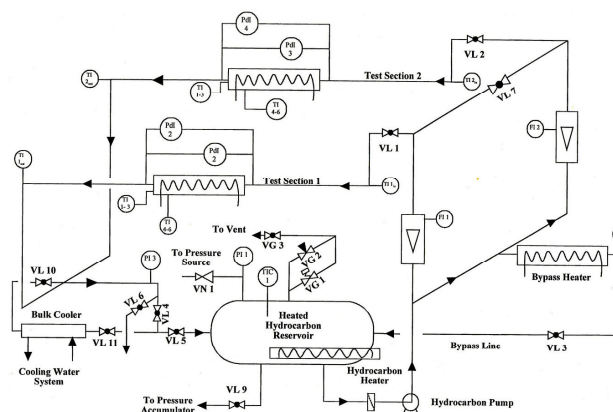


Fig. 1 Schematic of the pilot-scale parallel tube apparatus (Phillips, 1999)

The apparatus comprised a 0.105 m³ heated reservoir, a variable speed centrifugal feed pump and a by-pass for circulating crude oil through the reservoir whilst the oil was being heated. Flow rates to two 270 mm parallel tubular test sections were individually controlled and monitored using rotameters. Three surface thermocouples were used to record tube surface temperatures. The apparatus was maintained at a constant pressure of 15 bar and the crude oil temperature was maintained constant at 150°C. Surface temperatures up to 280°C were obtained by constant flux direct electrical heating.

Unfiltered Maya crude oil was selected for study since it was expected to foul easily and because it contained a low percentage of light ends, making it easier to handle in the laboratory (Crittenden et al., 2009). The overall composition of Maya crude oil and its physical properties are provided elsewhere (Phillips 1999; Crittenden et al., 2009). Typical properties were 21.1 API gravity, vapour pressure in the range 6.2-6.7 psig, 0.55% gas w/w, 4.03% total wax w/w, -21°C pour point, a calculated cloud point in the range 17-40°C, and viscosities of 161.5 and 54.80 mm²/s at 30°C and 50°C, respectively. Fluid properties were assumed to remain constant from run to run.

The hiTRAN[®] tube inserts were provided by Cal Gavin Ltd (Alcester, UK; www.calgavin.com). Most experiments were conducted using a “medium density” insert signified as MDI in Table 1. The medium density insert consisted of about 420 wire loops per metre, each loop being of 12.2 mm diameter and made from 0.76 mm diameter stainless steel wire. The loop matrix occupied the entire test section. Figure 2 illustrates the configuration of a tube fitted with inserts.



Fig. 2 Tube fitted with inserts
(Courtesy of Cal Gavin)

CFD SIMULATION

The Comsol Multiphysics package Version 4.1 (Comsol Burlington, MA, USA) is used to model the temperature and velocity fields in bare tubes as well as in tubes fitted with the insert. The equations of the $k-\epsilon$ turbulence flow model can be found elsewhere (Comsol Model Library, 2006; Yang et al., 2009). **For both the bare tube and the tube fitted with the insert, the geometries are taken to be three-dimensional.** The hiTRAN[®] inserts comprise a series of loops equally spaced with a helical pattern and a periodical pattern in the axial dimension. For CFD simulation, the inserts are represented by closed round loops whose diameter and thickness are set to be the same as for the actual insert. The loops are placed in a cylinder so that the actual situation is closely simulated. Details of the model

geometry for the tube with inserts are described in a later section.

The physical model used for the simulation is non-isothermal turbulent flow with conjugated heat transfer. The boundary conditions are set to be a logarithmic wall function for all walls, a constant linear velocity for the inlet and an open boundary for the outlet. The simulations were conducted for average inlet velocities in the range of the experimental conditions shown in Table 1. Under the conditions listed in Table 1, the fluid flow in the tube with inserts is in turbulent mode according to the study by Ritchie et al. (2009). The mesh size at the boundaries was set to be much smaller than in the bulk fluid. A series of simulations was conducted, beginning with a coarse mesh and then refined until the resulting velocity field and the velocity gradient near the wall were virtually independent of the mesh size. Further mesh refining caused significantly longer computational times. The boundary conditions for heat transfer are described later. The Reynolds numbers shown in Table 1 were calculated for a bulk temperature of 150°C and neglected the presence of the insert.

Table 1 Experimental Conditions

Velocity (m/s)	Re	Initial (clean) surface temperature	
		250°C	265°C
0.5	3600	Bare & MDI	Bare & MDI
0.8	5800	Bare	NA
1.0	7300	Bare & MDI	Bare & MDI
1.5	11000	Bare & MDI	Bare & MDI
2.0	14500	Bare & MDI	Bare
3.6	21800	Bare	Bare

RESULTS AND DISCUSSION

Detailed experimental results can be found elsewhere (Phillips, 1999; Crittenden et al., 2009), The CFD simulation results of the velocity field and the wall shear stress distribution are reported elsewhere (Yang and Crittenden, 2011) and hence only the results concerning the heat transfer coefficients are reported in this paper.

CFD simulation for heat transfer in a bare tube

The CFD simulation for the bare tube is straightforward. Figure 3 shows the resulting temperature field for the crude flow in a tube of 19.5 mm inside diameter, 2.5 mm thickness, and 0.25 m in length.

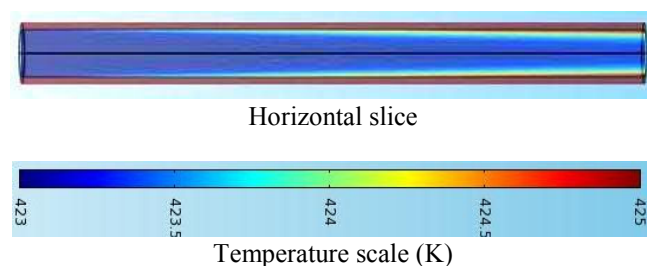


Fig. 3 Temperature distribution in the fluid flow inside a bare tube

The flow enters from the left hand side on Figure 3 and the CFD simulation conditions are as follows: an inlet velocity of 1 m/s, an inlet temperature of 423K and an outer wall temperature of 523K. A simple method has been developed to calculate the heat transfer coefficient based on the temperature distribution. Assuming a small portion of fluid in an annulus of diameter r , thickness Δr , and unit height passes a distance L from the bottom to the top as shown in Figure 4, the amount heat gained by this fluid portion is given by:

$$\Delta q = c_p \rho v 2\pi r \Delta r (T_{tr} - T_{br}) \quad (1)$$

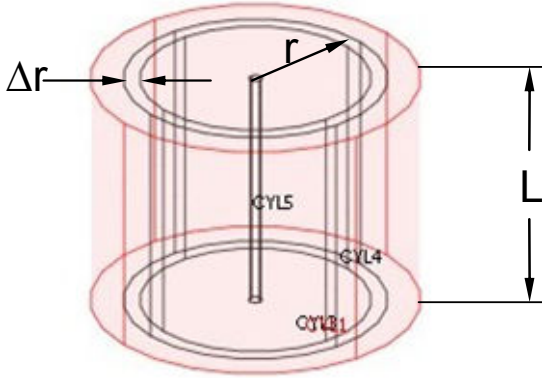


Fig. 4 Diagram for calculation of an average heat transfer coefficient

In this equation T_{tr} and T_{br} are the temperatures at the top (radius r) and bottom (radius r), respectively, and v is the linear velocity. The total heat obtained by the fluid contained in a cylinder of radius R and unit height is therefore given by:

$$q = c_p \rho v 2\pi \int_0^R r (T_{tr} - T_{br}) dr \quad (2)$$

In practice, the calculation is conducted by numerical integration, given that T_{tr} and T_{br} are results obtained from the model simulation. Figure 5 shows a typical radial temperature profile for a bare tube with an inlet velocity of 1 m/s, an inlet temperature of 423K and an outer wall temperature of 523K.

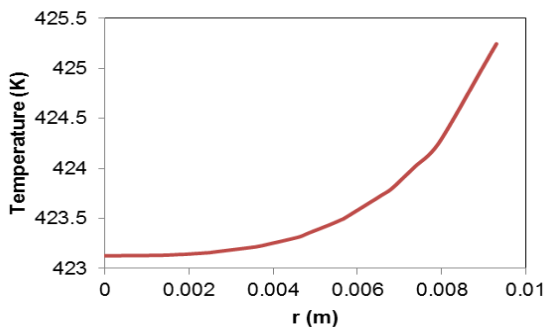


Fig. 5 Typical temperature profile over radius in a bare tube (axial distance $z = 0.2\text{m}$)

The heat transfer coefficient can then be calculated as follows:

$$h = \frac{q}{2\pi RL(T_s - T_b)} \quad (3)$$

Here T_s and T_b are the temperatures at the surface and in the bulk fluid, respectively, which are assumed to be constant. Table 2 shows a comparison of the average heat transfer coefficients obtained by simulation, from the Dittus-Boelter equation, and from experiments. The method for calculation of the heat transfer coefficient based on the experimental measurements of the inlet and outlet temperatures can be found elsewhere (Phillips, 1999). The Nusselt and Reynolds numbers shown in Table 2 are those for the experimental data (Phillips, 1999). The Table reveals that the simulated values of the heat transfer coefficient ($\text{W/m}^2\text{K}$) are in broad agreement with the experimental values.

Table 2 Average heat transfer coefficient for bare tube

Velocity (m/s)	h by simulation	h by Dittus-Boelter method	h Experimental value (Phillips 1999)	Re	Nu
0.5	443	391	490	4813	101
1.0	826	682	780	9627	176
2.0	1365	1186	1280	19253	306

CFD simulation for heat transfer in a tube fitted with an insert

Because of the inserts, the axial symmetry assumption cannot be used and so the fluid flow and heat transfer has to be modelled in a three dimensional geometry. The insert loop significantly increases the number of mesh elements and therefore the number of loops to be considered must be kept to as few as possible. Given its periodical pattern, as seen in Figure 2, the number of loops is taken in such a way that the periodical pattern repeats just once. The fluid flow pattern, including the shear stress, would be expected to repeat periodically along the axial direction.

For the simulation, the whole tube is divided into three sections, namely pre-insert (insulated), insert, and post-insert (insulated) sections as shown in Figure 6. The boundary conditions for all walls of the solid domains/metal phases in the pre- and post- insert sections are set to be as for thermal insulation. The outer wall in the insert section is set to be at constant temperature (250°C or 523K), and the inner wall to be a thermal wall function. This arrangement would simplify the calculation of the average heat transfer coefficient using the temperature distributions obtained from the simulation. Firstly, due to the mixing effect, the temperature field at a radial section can be considered to be of axial symmetry at a sufficient horizontal distance from the insert section. Secondly, the heat gained by the fluid contained in an imaginary cylinder of radius R and unit height, which is moving from the far left to the far right, is solely from the insert section, and hence the surface area involved in the heat transfer is limited to that of the insert

section, that is, the height of the wall in Equation 3 is fixed to be the length of the insert section.

Figure 6 shows the temperature field. It is notable that the fluid temperature is higher at the location just behind the wire loop, where the shear stress is lower according to Yang and Crittenden (2011). The plot of fluid temperature at a distance of 0.002 m away from the wall surface against shear stress is shown in Figure 7. It indicates that there is a negative correlation between these two parameters, though it is a somewhat weak one. Given the known influences of shear stress and temperature on fouling, fouling is more likely occur on the wall just behind the wire loop that touches the surface.

The effect of an insert on particles flowing in a liquid stream has been demonstrated by Cal Gavin in their laboratory. Fine particles move with the fluid, but some settle down just behind the wire loops where they touch the surface, and where shear stress is lower. This demonstrates an important effect of shear stress on fouling. The effects of both wall surface temperature and the film temperature (which is simply an average of wall and bulk temperatures) have both been used in previous fouling research investigations. Nonetheless, little attention has actually been paid to the effect of the local fluid temperature near to the wall. This local fluid temperature near wall may play an important role in the crude oil fouling process, as it can have a significant influence on the phase behaviour of asphaltenes present in the oil, a phenomenon believed to be a key aspect of the crude oil fouling process (Macchietto et al. 2011). Unfortunately, no experimental results are available to demonstrate the effect of fluid temperature near the wall on fouling either in the case of bare round tubes or tubes fitted with inserts.

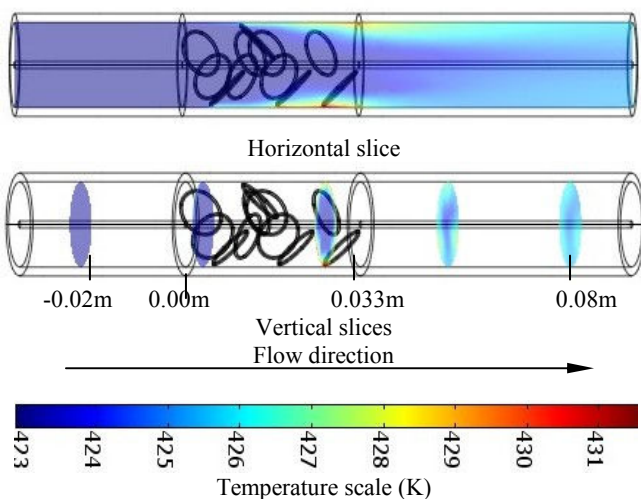


Fig. 6 Temperature field in a tube fitted with inserts inlet linear velocity: 1m/s; bulk temperature: 423K

In theory, an average heat transfer coefficient can be calculated based on the heat transfer coefficient distribution, which is obtained from the CFD simulation. This is difficult in practice in the case of a tube fitted with an insert, given the complexity of the distribution of local heat transfer

coefficients over any repeating cycle along the surface. The average heat transfer coefficient is therefore calculated using the method described earlier. The inner wall temperature, T_s , which is required to calculate the average heat transfer coefficient, is obtained from the model simulation, as shown in Figure 8. In this case for an inlet velocity of 1 m/s, a tube wall thickness of 3 mm, and an outer wall temperature at the insert section of 523K, the inner wall temperature can simply be considered to be constant at 504.2K. In this figure, the temperature data are read at the locations from one loop/surface contact to the next at the same angular position. As seen in this figure, the wall temperature is slightly higher at the position where the wire touches the wall, which is likely due to the lower local heat transfer coefficient at such a location.

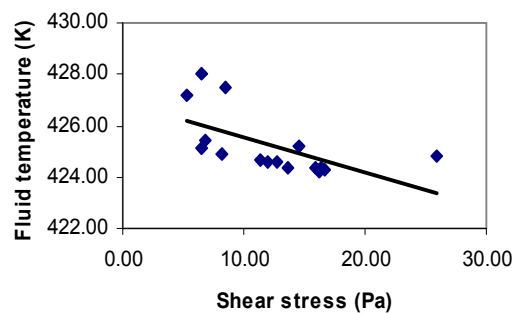


Fig. 7 Plot of local fluid temperature at near wall against local wall shear stress

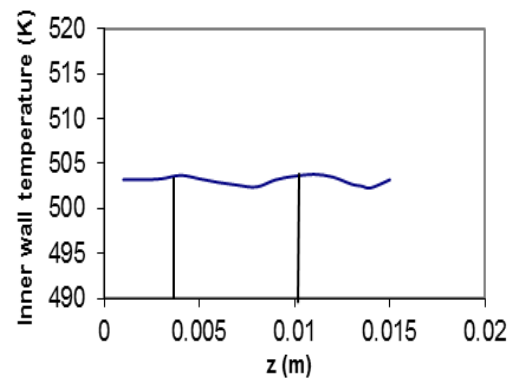


Fig. 8 Temperature distribution over the inner wall The vertical lines mark the contact position of the wire with the tube wall

Figure 9 shows that the temperature distribution for an average inlet velocity over the radius near the left end, that is in the pre-insert section at $z = -0.02m$, is essentially constant, as expected. Figure 10 shows the temperature distribution for the same average inlet velocity over the radius near the right hand end of the insert section, that is at $z = 0.08m$. It should be noted that at this location the temperature distribution is almost axially symmetric, with a smooth profile across the radius, with only 1.6 K difference from the centre to wall.

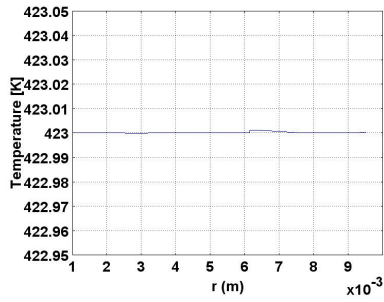


Fig. 9 Temperature distribution over radius
Outer wall temperature at insert section: 523K
Inlet temperature: 423K

Based on the temperature distributions, the average heat transfer coefficients are calculated using Equations 1-3, and the results together with those obtained from experiments for both the bare tube and the tube fitted with an insert are shown in Table 3. These data indicate that the simulation results are in fair agreement with the experimental data, thereby helping to confirm that the predicted local values of temperature and heat transfer coefficient (W/m^2K) are accurate. The data shown in Table 3 also indicates that the insert significantly increases the average heat transfer coefficient when the bulk velocity is kept constant at 1 m/s.

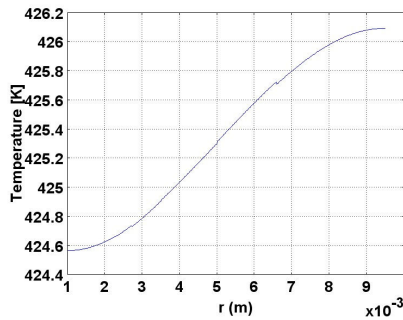


Fig. 10 Temperature distribution over radius
Outer wall temperature at insert section: 523K
Inlet temperature: 423K

Table 3 Average heat transfer coefficient for tube fitted with insert

Velocity (m/s)	h	h	h
	Bare tube experimental value Phillips (1999)	Tube with insert experimental value Phillips (1999)	Tube with insert by CFD simulation
0.5	490	1460	1644
1.0	780	2150	2292
2.0	1280	3460	3768

The increase in the heat transfer coefficient when an insert is used means that the temperature in the shell side of an exchanger can be reduced for a given thermal duty, so helping to reduce the fouling potential.

It is interesting to plot the local surface temperature over the wall as a function of the local shear stress, and to compare this plot with the fouling threshold conditions

reported elsewhere by Yang and Crittenden (2011). As seen in Figure 11, the local conditions of surface temperature and surface shear stress fall in the fouling zone for operation at an outer wall temperature of 523K and an average inlet velocity of 1 m/s. In contrast, the local conditions fall within the non-fouling zone for the same outer wall temperature but at the higher average velocity of 3.6 m/s. These results are confirmed by the experimental results (Phillips, 1999) in which fouling did occur at this surface temperature with an average velocity of 1 m/s for the tube fitted with a mid density insert. The experimental results also showed that fouling occurred for the bare tube at this temperature and an average velocity of 3.6 m/s, though no experimental results were obtained under these conditions for the tube fitted with the insert. These results indicate that the simulation is indeed able to help in identifying the appropriate operational conditions to eliminate or reduce fouling by taking into account the detailed local conditions.

The variation of local velocity or turbulent shear stress over the wall may have some influence on the local heat transfer coefficient. An example of this is shown in Figure 12 which shows that there is a slightly positive correlation between the local heat transfer coefficient and the local shear stress. In this plot the average velocity is 1 m/s, the inlet temperature is 423K and the outer wall temperature is 523K.

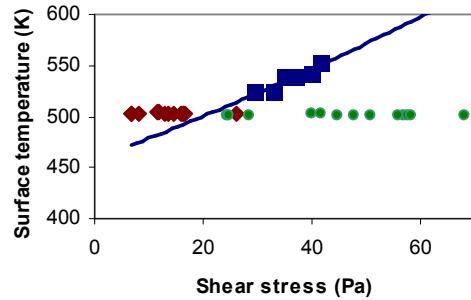


Fig. 11 Plot of local surface temperature against local shear stress in the plane of fouling threshold conditions

◆: inlet velocity 1 m/s; ●: inlet velocity 3.6 m/s
Inlet/Bulk temperature: 423K
Outer wall temperature: 523K
■: threshold conditions (Yang and Crittenden, 2011) converted to shear stress from equivalent velocity

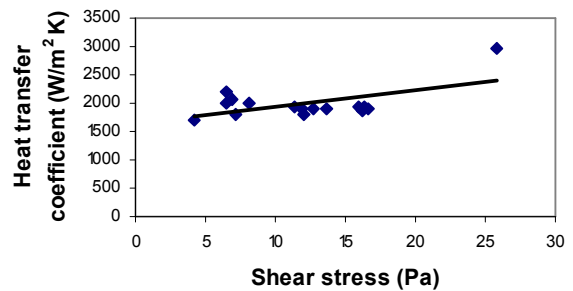


Fig. 12 Local heat transfer coefficient as a function of the local shear stress

CONCLUSION

1. CFD simulation has been conducted to investigate the effect on fouling of fitting a hiTRAN[®] insert into a round tube. The simulation reveals that the local wall temperature is higher behind the edge of the insert loop than elsewhere.
2. The higher local temperature and lower shear stress could prompt fouling in this particular location.
3. The simulation also confirms that the average heat transfer coefficient of a tube fitted with an insert is much higher than the bare tube operated under the same conditions of surface wall temperature and average velocity.
4. The method for predicting the average heat transfer coefficient using CFD simulation can be valuable in providing critical information on the design of a heat exchanger which comprises tubes fitted with inserts.
5. The CFD and heat transfer simulation provides a valuable tool in studies of the effect on fouling of the local fluid temperature near the wall. This is especially the case for tubes fitted with inserts or other with other types of irregular geometry.

ACKNOWLEDGEMENTS

The authors are grateful to the UK's Engineering and Physical Sciences Research Council (EPSRC) for the award of research grant EP/G059497/1 to study intensified heat transfer for energy saving in the process industries, and to the European Commission for the award of research grant FP7-SME-2010-1-262205-INTHEAT to study intensified heat transfer technologies for enhanced heat recovery. The authors are also grateful to project partners at the University of Manchester, and to Cal Gavin Ltd for their support, advice and provision of data for their hiTRAN[®] inserts.

NOMENCLATURE

- c_p specific heat capacity, kJ/(kg K)
 h heat transfer coefficient, W/(m² K)
 L tube section length used for calculation of h , m
 q heat, J
 r radial coordinate, m
 R inner radius of the tube, m
 Re Reynolds number
 T_b bulk temperature, K
 T_s surface temperature, K
 T_{br} temperature at bottom for calculation of h , K
 T_{tr} temperature at top for calculation of h , K
 z axial coordinate, m
 ρ fluid density, kg/m³
 \mathbf{v} average inlet fluid velocity, m/s

REFERENCES

- Bott, T. R., 2001, Potential physical methods for the control of biofouling in water systems, *TransIChemE, Part A*, Vol. 79, pp. 484-490.
Comsol Model library - Chemical Engineering Module, 2006, pp. 230-231.

Crittenden, B. D., Kolaczowski, S. T. and Takemoto, T., 1993, Use of in-tube inserts to reduce fouling from crude oils, *AIChE Symp. Series*, Vol. 89 (No. 295), pp. 300-307.

Crittenden, B. D., Kolaczowski, S. T. and Phillips D. Z., 2009, Crude oil fouling in a pilot-scale parallel tube apparatus, *Heat Transfer Engineering*, Vol. 30 (10-11), pp. 777-785.

Krueger, A. W. and Pouponnot, F., 2009, Heat exchanger performance enhancement through the use of tube inserts in refineries and chemical plants – successful application examples: Spirelf, Turbotal and Fixotal systems. *Proc. Eurotherm Conference on Fouling and Cleaning in Heat Exchangers*, Schlading, Austria, pp. 400-406.

Macchietto, S., Hewitt, G. F., Coletti, F., Crittenden, B. D., Dugwell, D. R., Galindo, A., Jackson, G., Kandiyoti, R., Kazarian, S. G., Luckham, P. F., Matar, O. K., Millan-Agorio, M., Müller, A., Paterson, W., Pugh, S. J., Richardson, S. M. and Wilson, D. I., 2011, Fouling in crude oil preheat trains: a systematic solution to an old problem, *Heat Transfer Engineering*, Vol. 32, 197–215.

Phillips, D. Z., 1999, Mitigation of crude oil fouling by the use of hiTRAN inserts, Ph.D thesis, University of Bath.

Ritchie, J. M. and Droegemueller, P., 2008, Application of tube inserts in heat exchangers: benefits of tube inserts, in *Heat Exchanger Design Handbook*, Ed. G. F. Hewitt, Begell House, Redding, CT, Section 3.21.2.

Ritchie, J. M., Droegemueller, P. and Simmons, M. J. H., 2009, hiTRAN[®] wire matrix inserts in fouling applications, *Heat Transfer Engineering*, Vol. 30, pp. 876-884

Wills, A., Bott, T. R. and Gibbard, I. J., 2000, The control of biofilms in tubes using wire-wound inserts, *Canadian J. Chem. Eng.*, Vol. 78, pp. 61-64.

Yang, M. and Crittenden, B. D., 2011, Fouling thresholds in bare tubes and tubes fitted with inserts, *Applied Energy*, in press.

Yang, M., Young, A. and Crittenden, B. D., 2009, Use of CFD to correlate crude oil fouling against surface temperature and surface shear stress in a stirred fouling apparatus, *Proc. Eurotherm Conference on Fouling and Cleaning in Heat Exchangers*, Schlading, Austria, pp. 272 – 280.